Effect of Electrode Arrangements on EHD Conduction Pumping

Ichiro Kano, *Member, IEEE*, and Tatsuo Nishina

***Abstract*—An experimental investigation is conducted to develop an electrohydrodynamic (EHD) pump based on microelectromechanical systems technology. In EHD conduction pumping, Coulomb force is the main driving force for fluid motion. The nonequilibrium process of the dissociation and recombination of dielectric liquid, HFE-7100, produces heterocharge layers in the vicinity of the electrodes. The attraction between the heterocharge layers and electrode surfaces generates the net motion in the dielectric liquid by applying asymmetric electric fields. In order to generate the asymmetric electric fields, three electrode patterns were prepared. The working fluid was confined between two electrodes facing each other. The generated pressure was measured for the different asymmetric electric fields. Also, the effect of deviation between the upper and lower electrode patterns on the pressure was investigated. Finally, the liquid flow rate, power consumption, and pump efficiency were measured with an optimized electrode arrangement. It is clear from the experimental results that, in addition to the conduction pumping, the ion injection generated at the microelectrode edge increases the pressure.**

***Index Terms*—Conduction pumping, electrohydrodynamics, ion drag, micropumps, nonmechanical pump.**

I. Introduction

ELECTROHYDRODYNAMIC (EHD) pumping has the advantages of absence of moving parts, simple design, and low weight. For this reason, a number of theoretical and experimental investigations concerning this pump design have been widely pursued since the early 1960s [1]–[3].

A detailed review of the EHD mechanisms has been given in previous studies [4], [5]. The electric body force density can be expressed as

$$\mathbf{f} = q\mathbf{E} - \frac{1}{2}E^2\nabla\varepsilon + \nabla\left[\rho\frac{E^2}{2}\left(\frac{\partial E}{\partial \rho}\right)_T\right] \tag{1}$$

where q is the charge density, $\mathbf{E}$ is the electric field, ε is the liquid permittivity, ρ is the mass density, and $(\partial\varepsilon/\partial\rho)_T$ is determined at constant temperature T. The first term on the right-hand side of (1) is the Coulomb force, the second term is referred to as the dielectric force, and the third term is the electrostriction force. For single-phase incompressible isothermal dielectric liquids, the predominant mechanism for EHD pumping is the Coulomb force. There are two types of EHD pumping mechanisms using high dc voltage which are applied to dielectric liquids. The first is ion-drag pumping, in which ions are created at a high-curvature metal/liquid surface. The second method of generating space charge is through the bulk conduction of slightly conductive liquids [4]. In the absence of any injection process at the electrodes, heterocharge layers of finite thickness appear in the vicinity of the electrodes. In the heterocharge layers, the charges have polarities opposite that of the adjacent electrode.

The development of microelectromechanical systems techniques enables the fabrication of EHD devices with much lower voltage, because the Coulomb force is dependent on the electric field [see (1)]. A number of researchers have studied the use of the EHD force for pumping liquids in microsystems. Recently, the increase in the power density of advanced microprocessors and laser diodes has created the need for improved cooling technologies in order to achieve high heat-dissipation rates. The microfluidic systems driven by EHD pumps can enhance the convective cooling of electrical devices [8]–[11].

Ion-drag pumping is generally not desirable because it can deteriorate the electrical properties of the dielectric liquid and the electrode surface conditions. As a result, the pumping performance decreases for long-term driving. Kano *et al.* [12] reported that the static pressure generated by an ion-drag pump consisting of microscale electrodes decreased toward zero for several dozens of hours. In this case, most ions were injected near the edge of the positively energized electrodes. In order to improve the EHD pumping performance, including not only long-term driving but also high-pressure generation, we redesigned an arrangement of the previous microelectrode patterns according to the conduction pumping mechanism [13]. In this arrangement, the dielectric liquid was confined between a planar symmetric microelectrode and a plane surface electrode. The EHD conduction mechanism, however, relies primarily upon the asymmetric electrode configuration. For example, Siddiqui and Seyed-Yagoobi [14] conducted an experimental observation of dielectric liquid flow induced by dc electric fields on asymmetric electrodes. This study was later numerically simulated by Yazdani and Seyed-Yagoobi [15]. In addition, Kazemi *et al.* [16] tested a micropump assembled with the asymmetric electrode. They reported a significant increase in both the pressure generation and flow rate with the asymmetric electrode configuration compared with the symmetric electrode configuration.

Manuscript received July 1, 2011; revised January 23, 2012; accepted May 23, 2012. Date of publication January 21, 2013; date of current version March 15, 2013. Paper 2011-EPC-225.R1, presented at the 2011 IEEE Industry Applications Society Annual Meeting, Orlando, FL, USA, October 9–13, and approved for publication in the IEEE Transactions on Industry Applications by the Electrostatic Processes Committee of the IEEE Industry Applications Society. This work was supported by the New Energy and Industrial Technology Development Organization of Japan under Grant 06B44014a of the Industrial Technology Research Grant Program.

The authors are with Yamagata University, Yonezawa 992-8510, Japan (e-mail: kano@yz.yamagata-u.ac.jp; kano@yz.yamagata-u.ac.jp).

Color versions of one or more of the figures in this paper are available online at http://ieeexplore.ieee.org.

Digital Object Identifier 10.1109/TIA.2013.2241711

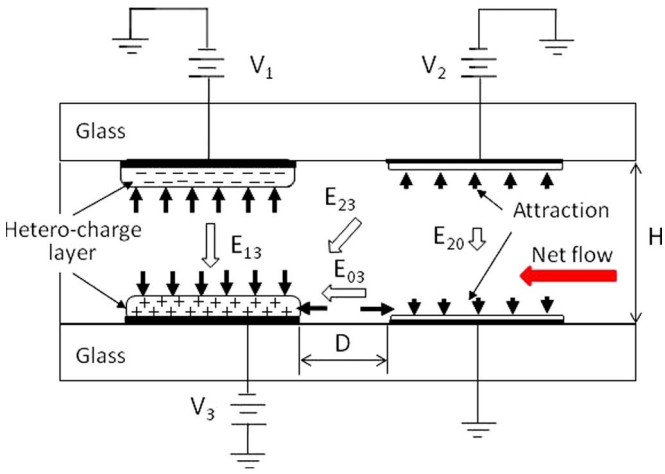

Fig. 1. Conduction pumping for the present electrode arrangement.

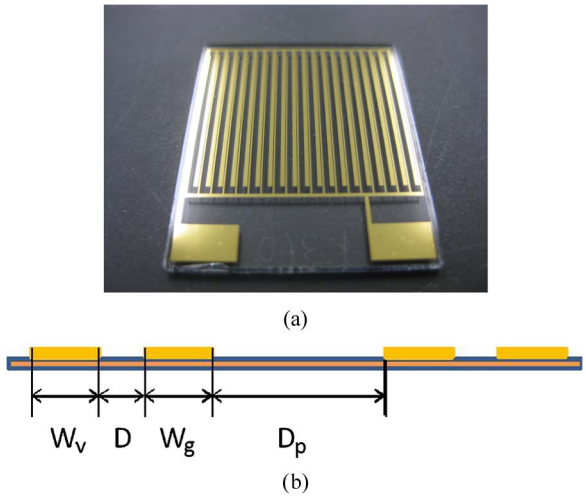

Fig. 2. Electrode pattern. (a) Photograph of the electrode pattern. (b) Electrode widths and spaces.

In this paper, we experimentally investigate the effect of the electrode geometry including the asymmetric electrode on the performance of conduction pumping in terms of static pressure, flow rate, and efficiency. Also, the effect of the deviation between the upper and lower electrode positions was investigated.

II. EHD Pumping Mechanism

Atten and Yagoobi [4] proposed a conduction pumping model of a needle- and a plane-shaped electrode in which the attraction between the electrodes and heterocharge layers induce the fluid motion near the electrodes. Under the low-electric-field regime, the conduction was mainly due to the positive and negative ions generated by dissociated molecules. When an electric field exceeding a certain threshold (on the order of 10 kV/mm, depending on the fluid characteristics) is applied, the rate of dissociation exceeds that of the recombination. As a result, the heterocharge layer on the liquid side is created away from the electric double layer. In the heterocharge layer, charges have polarities opposite that of the adjacent electrode. The heterocharge layer will begin to move when the layer experiences the electric field, while the ions on the electric double layer are fixed and immobile. Thus, the motion around the high-voltage electrode can mainly contribute to the net axial flow for the needle.

We designed an arrangement of the microelectrode patterns according to the conduction pumping mechanism. Fig. 1 shows the illustration of the present electrode arrangement. The applied voltages V_1 and V_2 are positively energized at the same value, and V_3 is negatively energized. In this case, there are four principal electric fields in the working fluid: the electric fields between the microscale electrodes, $E_{03} = -V_3/D$; between the positively and negatively energized microelectrodes, $E_{23} = (V_2 - V_3)/\sqrt{D^2 + H^2}$; between the ground and the facing positively energized microscale electrodes, $E_{20} = V_2/H$; and between a positively energized microscale electrode and a facing negatively energized microscale electrode, $E_{13} = (V_1 - V_3)/H$. When the electrodes are charged, the conduction occurs due to the positive and negative ions generated by the dissociation of liquid molecules under the high electric field regime of E_{13}. The charged surface attracts counter-ions and repels co-ions (on dielectric liquid side), thereby forming the heterocharge layer away from the electric double layer. If the electric fields E_{03} and E_{23}, which have components parallel to the electrode plate, are applied, Coulomb forces are exerted on these mobile ions and the electromigration of the heterocharge layer drags the bulk fluid through viscous interaction.

TABLE I
Specifications of the Electrode

Wr =Wg/Wv	Wv [μm]	Wg [μm]	D [μm]	Dp [μm]	N [μm]
0.3	360	120	60	480	20
1.0	120	120	60	480	26
3.0	120	360	60	480	20

III. Experimental Apparatus

In this paper, three different electrode patterns were designed with an array of planar-comb-finger electrodes. A photograph of an electrode is shown in Fig. 2, and the specifications of the electrode are listed in Table I. Electrodes of the same width, $Wr = 1.0$, and two electrodes of different widths, $Wr = 0.3$ and 3.0, were prepared in this experiment. The electrodes that make up each pair were separated by a gap of 60 μm. The gap between electrode pairs was 480 μm. The patterned area was 14.3×18 mm^2, allowing for the fabrication of 20 electrode pairs with $Wr = 0.33$ and 3.0 and 26 electrode pairs with $Wr = 1.0$. The electrodes were fabricated on a glass plate of $25 \times 21 \times 1$ mm^3. Chromium (800-Å) and gold (3000-Å) thin films were deposited over the entire substrate. The wet-etching process was used to etch the Cr/Au electrodes. First, a photoresist coating was applied on top of the Cr/Au film, and the coating was then patterned by photolithography. Next, the photoresist was developed in a standard developer. Finally, the remaining photoresist was rinsed off after etching the Cr/Au film. The current flowing through the dielectric liquid is strongly affected by the impurities on the electrode surface

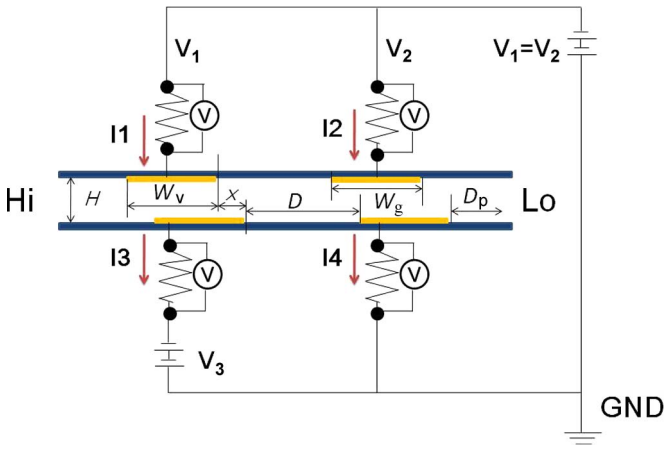

Fig. 3. Electrode layout.

TABLE II
PROPERTIES OF THE WORKING FLUID

Property	HFE-7100
Electric conductivity (S/m)	7×10^{-10}
Liquid density (kg/m^3)	1,520
Liquid kinematic viscosity (cSt)	0.38
Dielectric strength (kV/mm)	11
Dielectric constant	7.4

because the impurities behave as the ions in the liquid. Also, the pressure generated by the Coulomb force is strongly affected by the impurities. In order to remove the impurities, the electrode was immersed in sulfuric acid for 5 min. Then, hydrogen peroxide was added to the sulfuric acid. Finally, the electrode was washed with pure water. The working fluid was confined between the micropatterned electrodes, as shown in Fig. 3. The assembly was completed in a class 100 clean room using a two-sided adhesive tape (Nitto Denko HJ-3160), the thickness of which was 100 μm, to create a channel. HFE-7100 (3M) was used as the working fluid in the experiments. This liquid has a relative dielectric constant of 7.4 and relatively low viscosity. The other properties of this fluid are listed in Table II.

DC voltages V_1, V_2, and V_3 were applied to the electrodes by two high-voltage power supplies (Matsusada Model HEOPS-5B6) with a measurement uncertainty of $\pm$10 V. Under the present experimental conditions, a maximum voltage difference of 1000 V was applied to the working fluid. In the present experiment, the dc voltages of V_1 and V_2 were fixed at 500 V and that of V_3 was changed from -500 to 0 V. In order to investigate the effect of the deviation x between the upper and lower electrode patterns on the static pressure, x was changed from $-$ 10 to 60 μm with a measurement uncertainty of ±1 μA.

A photograph of the packaged micropump is shown in Fig. 4. The overall dimensions of the EHD pump were $30 \times 30 \times 5.3$ mm^3. The pumping channel dimensions were $21 \times 16 \times 0.1$ mm^3, and the main body of the pump was made of acrylic resin.

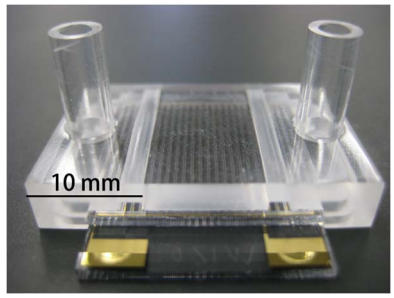

Fig. 4. Photograph of the micropump.

Two apparatuses were used to measure the static pressure and flow rate. Outline drawings of these apparatus and an explanation for static pressure and flow rate were illustrated in detail in [13]. The static pressure (zero flow rate) was measured using a digital differential pressure gauge (Okano Works Model DMP302N) with a measurement uncertainty of ±1 Pa, and the flow rate against the pressure load was measured using a film flowmeter (HORIBA STEC Model VP-2U) with a maximum measurement uncertainty of $\pm1.0\%$. The current flowing to the dielectric liquid is measured in terms of the voltage difference of a resistance of 100 kΩ with a measurement uncertainty of $\pm$40 nA.

In order to reproduce the electrode surface conditions, fresh liquid was used for each experiment. All dielectric liquids are likely to contain water and tiny particles from contact with the atmosphere. Therefore, all experiments were performed inside a class 1000 clean room with controlled moisture content (19.0%) and temperature (295.55 $\pm$0.5 K).

IV. EXPERIMENTAL RESULTS

A. Time Variation of the Pressure and the Corresponding Current Generated by a Step Voltage

The behaviors of the static pressure and the currents after applying dc voltage at $V_1 = V_2 = 500$ V and $V_3 = -500$ V with $Wr = 1.0$ are shown in Fig. 5. Note that static pressure is generated from the ground electrodes to the energized microelectrodes (see Fig. 1). In this figure, the pressure shows a sudden increase and then reaches an equilibrium level. After 2 min, the pressure exhibits a quasi-steady state. The maximum pressure is 240 Pa. Fig. 5 also shows the behaviors of the corresponding currents I1, I2, I3, and I4. The currents reach an equilibrium level after 2 min. Current I3 is on the same order as the sum of I1 and I2. However, I2 is more than 2.5 times larger than I1, while current I4 shows a very small value. This means that most of the current flows go through the dielectric liquid from I2 to I3. This result leaves us a question because the current should flow from I1 to I3 with the dissociation process induced by the high electric field intensity of E_{13}, as shown in Fig. 1. Since a sharp disturbance appears in the behaviors of currents I1 and I2, we should consider that the discharge could occur at the edge of the energized microelectrode at which the high electric field is produced locally.

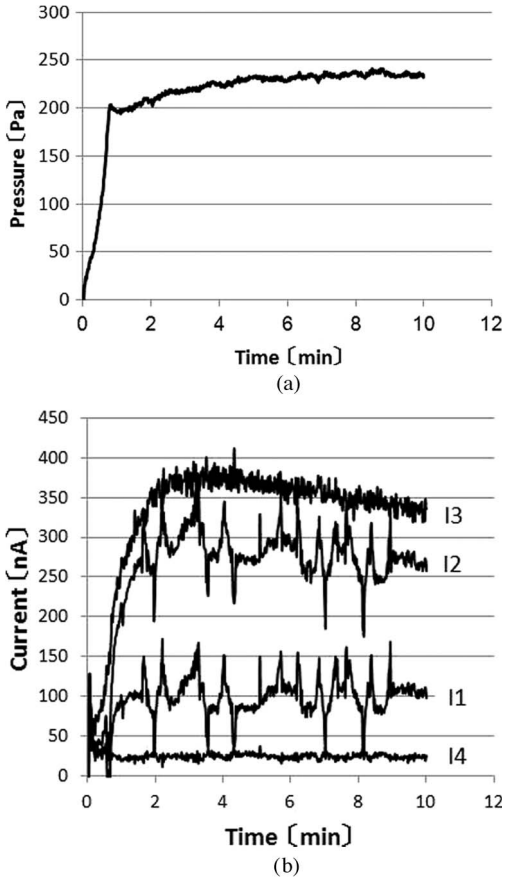

Fig. 5. Behavior of static pressure and corresponding current with $Wr = 1.0$ at $V_1 = V_2 = 500$ V and $V_3 = -500$ V. (a) Static pressure. (b) Corresponding current.

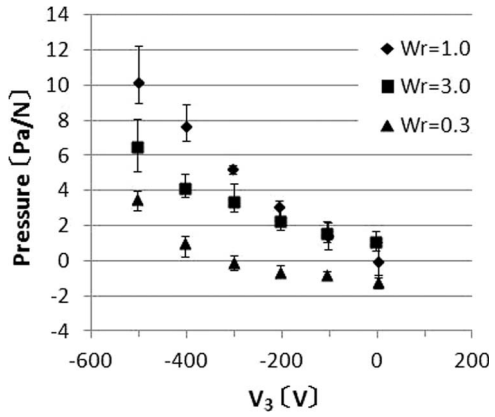

Fig. 6. Effect of the asymmetry electrode configuration on mean static pressure at $V_1 = V_2 = 500$ V.

B. Hydrostatic Behavior

The effect of the asymmetry electrode configuration on pressure is investigated. Fig. 6 shows the pressure generated by one electrode pair as a function of voltage V_3 at $V_1 = V_2 = 500$ V. The pressure was divided by the number of electrode pairs in order to compare the pressure generated by one electrode pair. The pressure at every W_r gradually increases with the decrease of voltage V_3. At $V_3 = -500$ V, the maximum pressures at $W_r = 1.0$, 3.0, and 0.33 are 10, 6.5, and 3.5 Pa/N, respectively. The difference between pressures with different asymmetric configurations shows a few pascals. It is clear that the pressure is not greatly influenced by the asymmetry electrode configuration, but the intensity of voltage V_3 strongly affects pressure intensity.

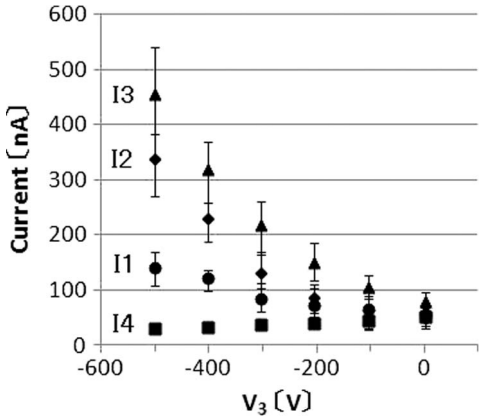

Fig. 7. Mean corresponding current with $Wr = 1.0$ at $V_1 = V_2 = 500$ V.

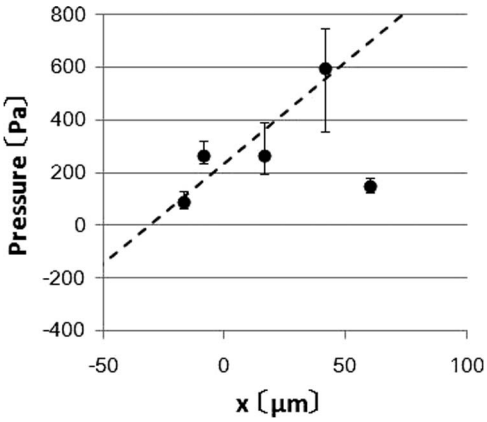

Fig. 8. Effect of the gap on the static pressure with $Wr = 1.0$ at $V_1 = V_2 = 500$ V and $V_3 = -500$ V.

The current behaviors with the symmetric electrode pattern $(Wr = 1)$ as a function of the applied voltage of V_3 at $V_1 = V_2 = 500$ V and $V_3 = -500$ V are shown in Fig. 7. The sum of I1 and I2 is equal to the sum of I3 and I4. Since the order of I4 is much smaller than the other currents, the sum of the input currents I1 and I2 almost exceeds I3. As shown in Fig. 5, it is interesting that the input current I2 is greater than I1 because the current should flow from I1 to I3 due to the high electric field intensity of E_{13}.

From these experimental results, the static pressure is correlated with the intensities of the current flows of I2 and I3. If ions are produced at the edge of the microelectrodes energized by V_2, the pressure could be strongly affected by electric field E_{23} (see Fig. 1) according to the Coulomb force. In order to investigate the effect of electric field E_{23}, the effect of the deviation x between the upper and lower electrode patterns on pressure is examined as follows.

The effect of the deviation x between the upper and lower electrode patterns on the pressure are shown in Fig. 8 at $V_1 = V_2 = 500$ V and $V_3 = -500$ V. From this figure, the pressure is strongly affected by the deviation x. As the deviation x is increased, the pressure rises from 100 Pa to a maximum of 600 Pa.

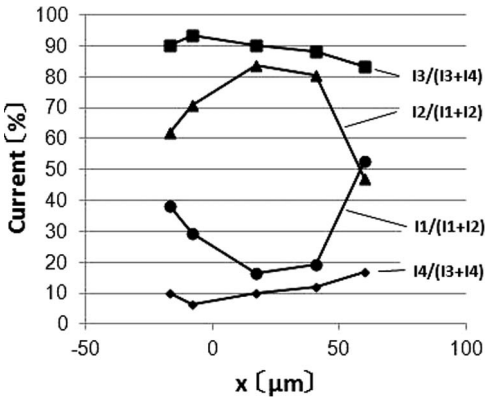

Fig. 9. Proportion of current flowing to electrodes with $Wr = 1.0$ at $V_1 = V_2 = 500$ V and $V_3 = -500$ V.

When x reaches 60 μm, which is the same as the electrode gap of Dp between the electrode pairs, the pressure suddenly decreases to 180 Pa.

The corresponding currents are shown in Fig. 9. The currents should be compared in relation to the total input or output currents, because the currents flowing through the dielectric liquid is strongly dependent on the impurities even if we carefully cleaned the electrodes and assembled the micropump in the clean room. The proportion of current I2 to the total input current I2/(I1 + I2) is increased with the increase of pressure. On the other hand, the proportion of current I1 to the total input current I1/(I1 + I2) is decreased with the increase of pressure. Currents I1 and I2 are much sensitive to the deviation.

As mentioned in the EHD pumping mechanism, the present EHD pump will produce the net flow under the conduction pumping mechanism in which the attraction between the electrodes and heterocharge layers induce a fluid motion. The heterocharge layer on the liquid side is created away from the electric double layer due to the positive and negative ions generated by dissociated molecules under the high electric field. It is, however, difficult to explain the present experimental results with only the conduction pumping mechanism. The behaviors of the pressure and current are affected by the ion injection generated at the edge of the electrodes. In fact, a sharp disturbance, which is caused by the local discharge, appeared in the behavior of the current at two energized electrodes, as shown in Fig. 5. In addition, the current mainly flows from the positively energized electrode of V_2 (I2) to the negatively energized electrode of V_3 (I3), as shown in Fig. 7. From these results, it is found that the ion injected at the edge of the positively energized electrode of V_2 increases the pressure.

C. Hydrodynamic Behavior

Fig. 10 shows the pressure load as a function of flow rate at the applied voltages of $V_1 = V_2 = 500$ V and $V_3 = -500$ V. The deviation x was set at 41 μm. The pressure load decreases linearly with the increase in flow rate. The maximum flow rate achieved is 2.6 mL/min without a pressure load.

Fig. 11 shows the corresponding currents I1, I2, I3, and I4 as a function of the flow rate. All currents increase linearly with the increase in flow rate. The current flowing to the ground

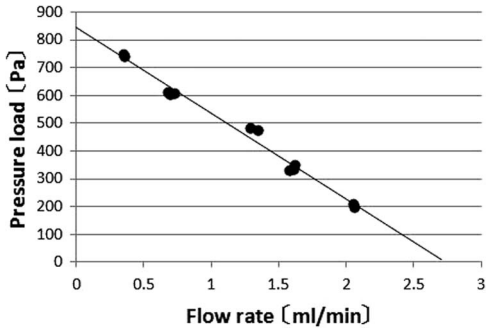

Fig. 10. Flow rate as a function of pressure load with $Wr = 1.0$ and $x = 41$ μm at $V_1 = V_2 = 500$ V and $V_3 = -500$ V.

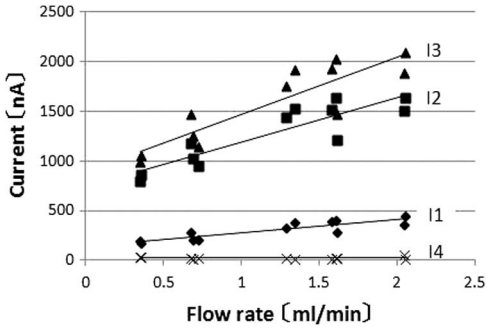

Fig. 11. Current as a function of flow rate with $Wr = 1.0$ and $x = 41$ μm at $V_1 = V_2 = 500$ V and $V_3 = -500$ V.

electrode, i.e., I4, is nearly zero. On the other hand, I2 and I3 are on the same order and much higher than I4. These results indicate that the current mainly flows from the positively energized electrode of V_2 (I2) to the negatively energized electrode of V_3 (I3). This behavior is the same as the static case.

In order to evaluate the dynamic performance of an EHD pump, we need to know the total current in order to determine the power consumption and efficiency. From Fig. 11, the current mainly flows from the positively energized electrodes of V_2 (I2) to the negatively energized electrodes of V_3 (I3). The pump power W and efficiency η were then calculated as follows:

$$\text{Pump efficiency}: \quad \eta = \frac{Q\Delta P}{W} \tag{2}$$

$$\text{Power consumption}: \quad W \approx \text{I2}(V_2 - V_3) \tag{3}$$

where Q is the flow rate, ΔP is the pressure load, $Q\Delta P$ is the generated mechanical power, and W is the power consumption (the applied electric power).

Fig. 12 illustrates the power consumption and pump efficiency. According to the figure, when the flow rate increased, the power consumption increased linearly to 2 mW at a flow rate of 2.0 mL/min and the pump efficiency decreased. The maximum pump power efficiency was 0.6% at a flow rate of 1 mL/min. Note that the EHD efficiency is usually low and that volumetric Joule heating is the primary cause of the low efficiency.

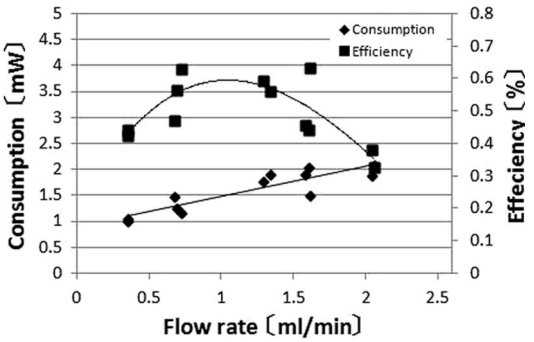

Fig. 12. Power consumption and pump efficiency with $Wr = 1.0$ and $x = 41$ μm at $V_1 = V_2 = 500$ V and $V_3 = -500$ V.

V. Conclusion

The arrangement of microscale electrode patterns assembled in the EHD pump has been tested in order to generate the asymmetric electric fields in the working fluid. The present electrode arrangement facilitated a high electric field, ensuring small size and weight, as well as low applied voltage. In accordance with the conduction pumping mechanism, the pressure and flow were induced by the electromigration of the heterocharge layer in the vicinity of the charged microelectrodes. The effect of the deviation between the upper and lower electrode patterns strongly affected the static pressure, while the asymmetric electrode configuration slightly affected the static pressure. The pressure was increased with the increase of the deviation up to 600 Pa. It was found that, in addition to the conduction pumping effect, the ion injected at the edge of the positively energized electrode increases the pressure when the deviation is increased. Finally, the dynamic pumping performance was tested. The EHD pump with the deviation of 41 μm produced a maximum dynamic pressure of 850 Pa and a maximum flow rate of 2.6 mL/min at $V_1 = V_2 = 500$ V and $V_3 = -500$ V (at a maximum electric field of 10 kV/mm applied in the present experiments). The maximum power consumption and pump efficiency were 2.0 mW and 0.6%, respectively.

Acknowledgment

The authors would like to thank M. Suzuki for his crucial support in performing the experiments.

References

[1] M. Stuetzer, "Ion drag pressure generation," *J. Appl. Phys.*, vol. 30, no. 7, pp. 984–994, Jul. 1959.
[2] W. F. Pickard, "Ion-drag pumping. I. Theory," *J. Appl. Phys.*, vol. 34, no. 2, pp. 246–250, Feb. 1963.
[3] W. F. Pickard, "Ion-drag pumping. II. Experiment," *J. Appl. Phys.*, vol. 34, no. 2, pp. 251–258, Feb. 1963.
[4] P. Atten and J. Seyed-Yagoobi, "Electrohydrodynamically induced dielectric liquid flow through pure conduction in point/plane geometry," *IEEE Trans. Dielect. Elect. Insul.*, vol. 10, no. 1, pp. 27–36, Feb. 2003.
[5] J. Seyed-Yagoobi, "Electrohydrodynamic pumping of dielectric liquids," *J. Electrostat.*, vol. 63, no. 6–10, pp. 861–869, Jun. 2005.
[6] I. Kano and I. Takahashi, "Improvement for pressure performance of Micro-EHD pump with an arrangement of thin cylindrical electrodes," *JSME Int. J. Ser. B*, vol. 49, no. 3, pp. 748–754, 2006.
[7] I. Kano, I. Takahashi, and T. Nishina, "Effects of moisture content in a dielectric liquid on electrohydrodynamic pumping," *IEEE Trans. Ind. Appl.*, vol. 45, no. 1, pp. 59–66, Jan./Feb. 2009.
[8] J. Darabi, M. M. Ohadi, and D. DeVoe, "An electrohydrodynamic polarization micropump for electric cooling," *J. Microelectromech. Syst.*, vol. 10, no. 1, pp. 98–106, Mar. 2001.
[9] J. Darabi and K. Ekula, "Development of a chip-integrated micro cooling device," *Microelectron. J.*, vol. 34, no. 11, pp. 1067–1074, Nov. 2003.
[10] J. Darabi and H. Wang, "Development of an electrohydrodynamic injection micropump and its potential application in pumping fluids in cryogenic cooling systems," *J. Microelectromech. Syst.*, vol. 14, no. 4, pp. 747–755, Aug. 2005.
[11] S. Moghaddam and M. M. Ohadi, "Effect of electrode geometry on performance of an EHD thin-film evaporator," *J. Microelectromech. Syst.*, vol. 14, no. 5, pp. 978–986, Oct. 2005.
[12] I. Kano, Y. Shii, and T. Nishina, "Development of an electrohydrodynamic micropump," in *Conf. Rec. 42nd IEEE IAS Annu. Meeting*, New Orleans, LA, USA, Sep. 2007, pp. 38–44.
[13] I. Kano and T. Nishina, "Electrode arrangement for micro-scale electrohydrodynamic pumping," *J. Fluid Sci. Technol.*, vol. 5, no. 2, pp. 123–134, 2010.
[14] M. A. W. Siddiqui and J. Seyed-Yagoobi, "Experimental study of pumping of liquid film with electric conduction phenomenon," *IEEE Trans. Ind. Appl.*, vol. 45, no. 1, pp. 3–9, Jan./Feb. 2009.
[15] M. Yazdani and J. Seyed-Yagoobi, "Electrically induced dielectric liquid film flow based on electric conduction phenomenon," *IEEE Trans. Dielect. Elect. Insul.*, vol. 16, no. 3, pp. 768–777, Jun. 2009.
[16] P. Z. Kazemi, P. R. Selvaganapathy, and C. Y. Chang, "Effect of electrode asymmetry on performance of electrohydrodynamic micropumps," *J. Microelectromech. Syst.*, vol. 18, no. 3, pp. 547–554, Jun. 2009.

Ichiro Kano (M'03) received the Ph.D. degree in mechanical engineering from Tokyo Institute of Technology, Meguro, Japan, in 2000.

He was an Engineer for two years with Bridgestone Corporation beginning in 1994. Following his industrial career, he joined the Department of Mechanical Systems Engineering, Yamagata University, Yonezawa, Japan, in 1996, where he is currently an Associate Professor. His research interests are the enhancement of heat transfer and mass transport with electrohydrodynamics. He is currently active in the development of microcooling systems consisting of microchannels and micropumps for high-heat-flux electric cooling applications.

Dr. Kano is a member of The Japan Society of Mechanical Engineers and the American Society of Mechanical Engineers.

Tatsuo Nishina received the B.A., M.A., and Ph.D. degrees from Tohoku University, Sendai, Japan, in 1981, 1983, and 1994, respectively.

In 1983, he was with Honda Engineering R&D Company, Ltd., where he was involved in developing rubber parts for vehicles. In 1984, he joined Tohoku University and then moved to Yamagata University, Yonezawa, Japan. His current interest is focused on electrochemical energy conversion and storage, particularly on the key technology for express-charging/discharging lithium secondary batteries.